Discontinuous anchoring transition and photothermal switching in composites of liquid crystals and conducting polymer nanofibers

M. V. Rasna,[1] K. P. Zuhail,[1] R. Manda,[2] P. Paik,[2] W. Haase,[3] and Surajit Dhara[1,*]

[1]*School of Physics, University of Hyderabad, Hyderabad 500046, India*

[2]*School of Engineering Sciences and Technology, University of Hyderabad, Hyderabad 500046, India*

[3]*Darmstadt University of Technology, Eduard Zintl Institute for Inorganic and Physical Chemistry, Petersenstrasse 20, Darmstadt 64287, Germany*

(Received 17 March 2014; revised manuscript received 25 April 2014; published 8 May 2014)

We prepared nanocomposites of a nematic liquid crystal and nanofibers of a conducting polymer (polyaniline). All the nanocomposites exhibit a discontinuous surface anchoring transition from planar to homeotropic in the nematic phase on a perfluoropolymer coated surface with a thermal hysteresis (≈5.3 °C). We observe a relatively large bistable conductivity and demonstrate a light driven switching of conductivity and dielectric constant in dye doped nanocomposites in the thermal hysteresis (bistable) region. The experimental results have been explained based on the reorientation of the nanofibers driven by the anchoring transition of the nematic liquid crystal. We show a significant enhancement of the bistable temperature range (≈13 °C) by an appropriate choice of compound in the binary system.

DOI: 10.1103/PhysRevE.89.052503 PACS number(s): 61.30.Hn, 61.30.Eb, 42.70.Df

I. INTRODUCTION

In liquid crystal displays (LCDs) appropriate alignment layers are used on the substrates for the uniform and defect free alignment of the director (average orientational direction of the molecules [1]). Based on the surface alignment layers liquid crystals (LCs) can show two stable molecular orientations, namely, planar (long axes parallel to the substrate) and homeotropic (long axes perpendicular to the substrate) [2]. These states are stable, and the switching between these two states in the cell is realized by applying electric or magnetic fields [3]. LCDs are monostable optical devices in the sense that the "on" state is maintained as long as the field is kept on, requiring a continuous power supply. Optical bistable devices are those in which two states with different transmissions can be obtained at the same applied field and temperature. There are several reports on the bistable orientation of nematic liquid crystals [4–13]. In the case of bistable electrical devices two states with different conductivities can be obtained simultaneously. These devices are ideal for switching and memory applications and have been demonstrated in both inorganic and organic materials [14–19]. It is known that liquid crystals can be used as a template to achieve self-assembly of carbon nanotubes [20–22], gold nanorods [23], quantum dots [24], and nanofibers [25]. In the case of elongated particles the long axes of the particles are orientationally ordered along the LC director. The degree of orientational ordering of the nanoparticles in the LCs can significantly change the anisotropic physical properties. By applying external fields the orientation of the LC molecules and hence the nanoparticles can be changed. However, they are also monostable because of the monostablity of the host medium (liquid crystal). In previous studies we have reported a discontinuous anchoring transition in a nematic liquid crystal from planar to homeotropic with a large thermal hysteresis on perfluoropolymer treated substrates [26,27]. Recently, the heat capacity and thermal diffusivity change of the discontinuous anchoring transition have also been reported [28,29]. We demonstrated the optical bistability and memory effects driven by laser light [30–33]. However, the possibility of achieving the bistable orientation of elongated nanoparticles and switching the orientation via the external field or temperature has remained unexplored. In this paper, we report on the liquid crystal conducting polymer nanofiber (PANI) composites that exhibit a discontinuous anchoring transition from planar to homeotropic and vice versa with a large thermal hysteresis in perfluoropolymer treated cells. We show that the anchoring transition is retained in the nanocomposite without affecting the thermal hysteresis (i.e., bistable temperature range). The orientational coupling of the PANI nanofibers in the liquid crystal medium is examined by measuring the low frequency dielectric constant and conductivity. Exploiting the enhanced conductivity in the bistable region, we demonstrate an electrical conductivity switching in the dye doped sample driven by light. Finally, we show that using the appropriate choice of compound from the homologous series, the bistable temperature range can be enhanced by more than double.

II. EXPERIMENT

Indium tin oxide coated (ITO) glass plates with a circularly patterned electrode are used to make experimental cells. The glass substrates are spin coated with the perfluoropolymer poly[perfluoro(4-vinyloxy-1-butene)], known as CYTOP (Asahi Glass Co. Ltd.), and cured for 30 min at 100 °C. Empty cells with 13.5 μm spacing were fabricated using two such glass plates. The liquid crystal used in the experiment is 4′-butyl-4-heptyl-bicyclohexyl-4-carbonitrile (CCN-47) and was obtained from Merck. It exhibits the following phase transitions: Cr 25.6 °C SmA 28.4 °C N 58.2 °C I. It shows a discontinuous planar to homeotropic anchoring transition with thermal hysteresis (≈5.3 °C) in CYTOP coated cells. The chemical structures of CYTOP and CCN-47 are shown in Fig. 1(a). Various physical characterizations of this liquid

*Corresponding author: sdsp@uohyd.ernet.in

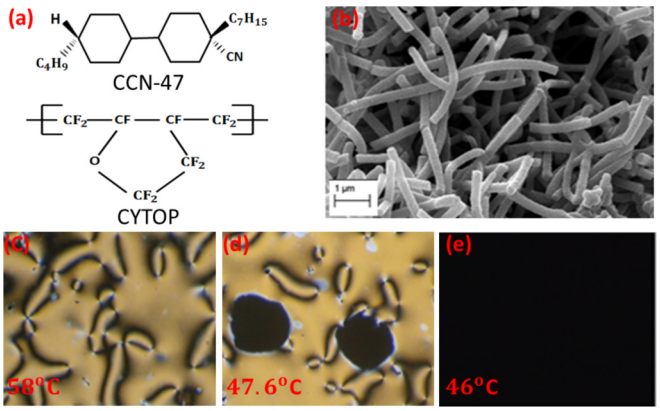

FIG. 1. (Color online) (a) Chemical structures of CCN-47 and CYTOP. (b) FESEM image of conducting PANI nanofibers. Photomicrograph of the textures showing the anchoring transition in CCN-47 under crossed polarizers: (c) CCN-47 at 58 °C, (d) CCN-47 at 47.6 °C, and (e) CCN-47 at 46 °C.

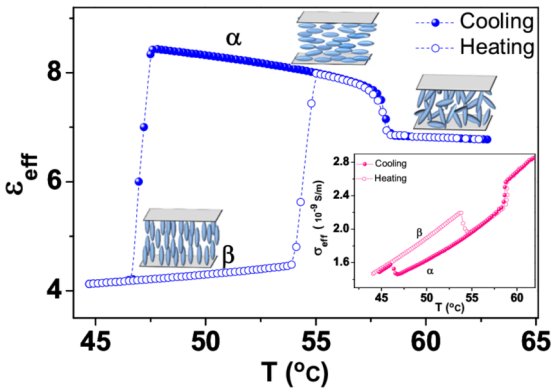

FIG. 2. (Color online) Temperature variation of the effective dielectric constant ($\epsilon_{\rm eff}$) and the effective conductivity ($\sigma_{\rm eff}$) in a CYTOP coated cell (inset). Applied voltage: 0.3 V, frequency: 100 Hz. Cell thickness is 13 μm. Molecular orientations at different temperatures are also schematically depicted.

crystal have already been reported [34–36]. The method of preparation of polyaniline (PANI) nanofibers has also been reported recently [37]. The length and diameter of the PANI nanofibers range from 1.5 to 11 μm and 100 to 250 nm, respectively [Fig. 1(b)]. PANI nanofibers are dispersed in chloroform and sonicated for 30 min for uniform suspension. Different concentrations of suspensions are added to the liquid crystal and mixed thoroughly by physical mixing, and then the solvent is evaporated very slowly (12 h). We found that the colloidal suspension of the nanofibers in the liquid crystal can be obtained with a maximum of 1.5 wt %, beyond which they tend to agglomerate. Hence we restricted our measurements to within 1.5 wt % of PANI nanofibers in the liquid crystal. It may be mentioned that this concentration is about 10 times larger than that reported previously in the case of pentyl cyanobiphenyl (5CB) [25]. After empty capacitance measurement, the sample was filled in the cell through capillary action. The dielectric properties were measured using an impedance analyzer (Novocontrol Alpha-A). All measurements were performed at a frequency of 100 Hz by applying 0.3 V (much less than the Fréedericksz threshold voltage) across the cell. The ac conductivity is calculated using the relation $\sigma_{||,\perp}(f) = 2\pi f \epsilon_o \epsilon''_{||,\perp}$ where ϵ_o is the permittivity of the free space and f is the frequency of the applied field. The subscripts refer to the directions in relation to the director. Considering the variation in the cell thickness and the standard deviation of the conductivity and dielectric data, our results are accurate within 3%. It may be mentioned that the conductivity anisotropy $\Delta\sigma$ $(=\sigma_{||} - \sigma_{\perp})$ of CCN-47 changes sign from positive to negative around 3 kHz frequency. The space charge polarization and electric double layer effects are observed below 10 Hz; hence we calculated conductivity from the imaginary part of the dielectric constant at 100 Hz in all the measurements.

III. RESULTS AND DISCUSSION

We show the textures observed under a polarizing optical microscope at various temperatures of CCN-47 in a CYTOP coated cell in Fig. 1. In the nematic phase a typical Schlieren texture with a few integer and mostly half defects are observed [Fig. 1(c)]. On cooling below 47.6 °C, a few small, dark regions grow abruptly and randomly [Fig. 1(d)]. The dark regions are domains [two dark spots seen in Fig. 1(d)] with homeotropic orientation of the molecules [26]. On further cooling, the whole sample becomes completely dark, suggesting a perfect homeotropic alignment of the molecules in the entire sample. This transition is discontinuous, and the width of the coexisting region is <1 °C. To investigate the change of molecular orientation from isotropic to planar and then to homeotropic, we measured the dielectric constant and conductivity of the sample as a function of temperature. The variation of both

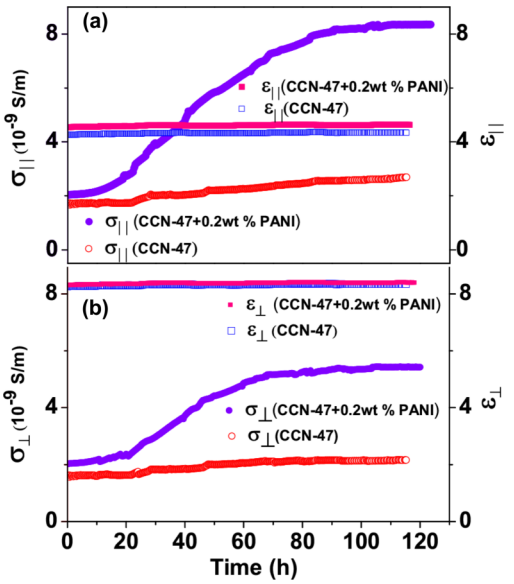

FIG. 3. (Color online) Time dependence of the dielectric constant and conductivity in the bistable region at 48 °C in CYTOP coated cells in a pure liquid crystal and in a nanocomposite with 0.2 wt % PANI nanofiber. The subscripts parallel (||) and perpendicular (⊥) correspond to the quantities measured in the homeotropic and planar states, respectively.

the effective dielectric constant and conductivity in CYTOP coated cells is shown in Fig. 2. Both the effective dielectric constant (ϵ_{eff}) and the effective conductivity (σ_{eff}) show a thermal hysteresis in the nematic phase. Comparing the dielectric constant reported in the literature for both planar and homeotropic cells [36], we find that in the hysteresis region (between 53.8 °C and 47.8 °C) $\epsilon_{\text{eff}} \approx \epsilon_{\perp}$ while cooling (state α) and $\epsilon_{\text{eff}} \approx \epsilon_{||}$ while heating (state β). These two states are stable with time. This is further verified from microscope observations and by measuring the dielectric constant and conductivity of the respective states with time at a fixed temperature. Figure 3 shows the variation of the conductivity and dielectric constant as a function of time in a pure liquid crystal as well as in a nanocomposite (with 0.2 wt % PANI). It is observed that the dielectric constants (both $\epsilon_{||}$ and $\epsilon_{\perp}$) remained almost constant, while the conductivities (both $\sigma_{||}$ and $\sigma_{\perp}$) increased with time and saturated after 3 to 4 days. Hence all our measurements are made after 5 days. A similar behavior of the conductivity was also observed in carbon nanotube dispersed liquid crystals, and it was attributed to the time dependent percolation of the nanotubes [38].

Figure 4(a) shows the temperature variation of ϵ_{eff} for all the nanocomposites. The nematic to isotropic (T_{NI}) transition and the anchoring transition temperatures are slightly increased. For example, T_{NI} increases about 1.4 °C when the concentration of PANI is increased to 1.5 wt %. All the nanocomposites exhibit thermal hysteresis, and the temperature range of the hysteresis remains almost unaffected. In Fig. 4(b) the variation of $\epsilon_{||}$ and $\epsilon_{\perp}$ with the concentration of PANI nanofibers at a fixed temperature (48.5 °C) is shown. It is observed that $\epsilon_{\perp}$ remains almost constant (≈8.5), while $\epsilon_{||}$ increases with the concentration of PANI nanofibers. For example, $\epsilon_{||}$ has increased from 4.3 to 5.5, showing an enhancement of about 20%. The dielectric anisotropy ($\Delta\epsilon = \epsilon_{||} - \epsilon_{\perp}$) in the bistable region is negative and has increased from −4.2 to −3 (inset). This suggests that the nanofibers are dielectrically anisotropic and the perpendicular component of the dielectric constant of the nanofibers is comparable to that of the liquid crystal i.e., $\epsilon_{\perp}^{\text{PANI}} \approx \epsilon_{\perp}^{LC}$, and the parallel component must be larger than that of a pure liquid crystal (i.e., $\epsilon_{||}^{\text{PANI}} > \epsilon_{||}^{LC}$).

The effect of the orientational coupling of nanofibers can be further investigated by measuring the effective conductivity of the nanocomposites since the nanofibres are made of conducting polymer (PANI). Figure 5(a) shows the temperature variation of the effective conductivity of various nanocomposites. The conductivity of the nanocomposites in the isotropic phase increases with the weight percent of the PANI nanofibers as expected. Figure 5(b) shows the variation of conductivity ($\sigma_{||}$ and $\sigma_{\perp}$) with concentration at a fixed temperature (48.5 °C). The conductivity anisotropy (the difference in conductivities between states α and β) at 100 Hz is positive and increases with the concentration of PANI nanofibers. For example, the conductivity anisotropies in pristine CCN-47 and in a nanocomposite (1.5 wt %) are ≈0.5×10^{-9} and ≈10.5×10^{-9} S/m, respectively (see the inset). Thus the conductivity anisotropy

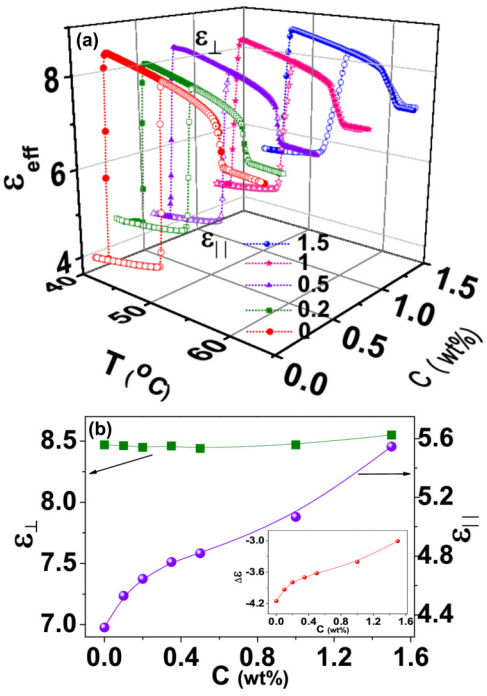

FIG. 4. (Color online) (a) Temperature variation of the effective dielectric constant (ϵ_{eff}) for various weight percent of PANI nanofibers. Only five different concentrations are presented for clarity. In the bistable region, $\epsilon_{\text{eff}} \approx \epsilon_{||}$ in the homeotropic state, and $\epsilon_{\text{eff}} \approx \epsilon_{\perp}$ in the planar state. (b) Variation of both dielectric constants in the bistable region at a fixed temperature (48.5 °C). The inset shows the variation of dielectric anisotropy $\Delta\epsilon$ with various weight percent of PANI nanofiber.

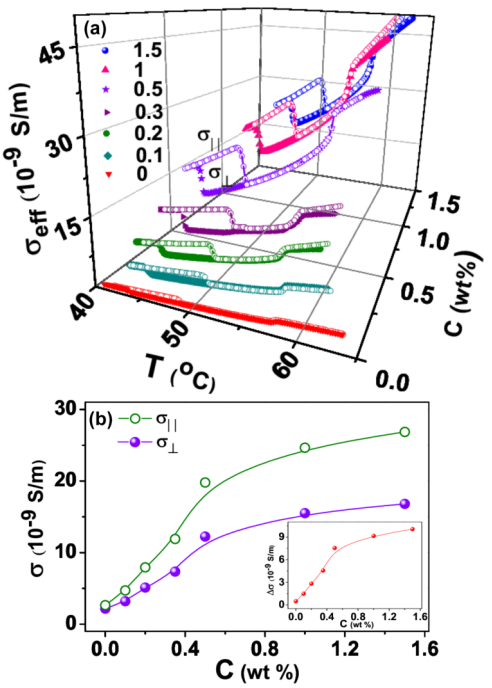

FIG. 5. (Color online) (a) Temperature variation of the effective conductivity (σ_{eff}) in the bistable regime for various weight percent of PANI in the nanocomposites. In the bistable region, $\sigma_{\text{eff}} \approx \sigma_{||}$ in the homeotropic state, $\sigma_{\text{eff}} \approx \sigma_{\perp}$ in the planar state. (b) Variation of the conductivity in the bistable region at a fixed temperature (48.5 °C). The inset shows the variation of the conductivity anisotropy $\Delta\sigma$ with various weight percent of PANI nanofiber.

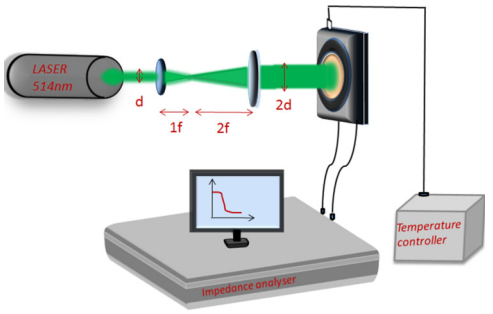

FIG. 6. (Color online) Diagram of the experimental setup for photothermal switching.

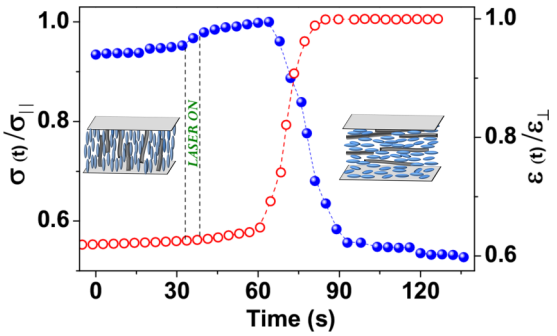

FIG. 7. (Color online) Time dependence of the normalized dielectric constant $[\epsilon(t)/\epsilon_{||}$; open red circles] and conductivity $[\sigma(t)/\sigma_{||}$; solid blue circles] in the bistable region under the action of laser. The duration of the laser irradiation is indicated between two vertical dotted lines. The schematic orientation of liquid crystal molecules and the nanofibers is also shown.

is enhanced nearly 20 times. Previously, we reported that the conductivity anisotropy is increased by about 10 times just by doping 0.2 wt % of PANI nanofibers in a 5CB liquid crystal [25]. We explained that such a large enhancement in $\sigma_{||}$ is due to the contribution of both the ionic and electronic conductivities.

Although the absolute values of both conductivities ($\sigma_{||}$ and $\sigma_{\perp}$) in the nanocomposites are much lower than the conductivity of pure PANI nanofibers [37], the relative enhancement of $\Delta\sigma$ in the composites is large compared to that of the pristine liquid crystal. Hence these nanocomposites can be used as biconducting materials in which two conductivities can be obtained simultaneously, and switching between them is possible by an appropriate external stimulus. Here we demonstrate a light driven switching of conductivity by doping a small amount (0.5 wt %) of laser dye [4-dicyanomethylene-2-methylene-2-methyl-6-(*p*-dimethylaminostyryl)-4H-pyran (DCM)]. A schematic diagram of the experimental setup is shown in Fig. 6. We used a tunable Ar-ion laser (130 mW) whose wavelength range falls in the absorption range of DCM. The light beam was expanded to illuminate the cell by an appropriate combination of lenses. First, the sample was cooled below 47 °C to obtain a homeotropic state (state β in Fig. 2); then it was heated up to 53 °C, which is just about 1 °C below the homeotropic to planar anchoring transition temperature. The cell is exposed to laser light for a few seconds (2–4 s), and the dye molecules absorb the light energy; as a result the temperature of the exposed area is increased. If the local temperature is greater than the anchoring transition temperature (homeotropic to planar), the molecules in the exposed area change orientation from the homeotropic to the planar state (state β to state α in Fig. 2, inset), and consequently, the conductivity decreases. In order to measure the response time, we measured the time dependent dielectric constant and conductivity for a duration before and after the irradiation using the impedance analyzer. The variation of the normalized dielectric constant $[\epsilon(t)/\epsilon_{||}]$ and conductivity $[\sigma(t)/\sigma_{||}]$ with time is shown in Fig. 7. After switching off the laser, the normalized conductivity quickly decreases to a lower value, while the normalized dielectric constant increases to a higher value, as expected. The representative models of the molecule and nanofiber orientation in two states are also shown in Fig. 7 (inset). The response time, i.e., the time within which the normalized conductivity decreases from the high to low value, is about 25 s. This is rather a slow response as the change in the molecular orientation is a photothermal process and switching time is limited by the heat transfer rate. It may be mentioned that the conductivity decay has two components, namely, the contributions from the director reorientation and also from the growth of the planar regions with time (after switching off the laser). At this stage we do not have much control over the latter process, which is expected to make the response slow.

For practical applications and also for fundamental studies it is necessary to have a wider range of bistability at lower temperature. In previous studies we reported that the anchoring transition temperatures can be lowered to room temperature in a binary mixture with positive dielectric anisotropy material [30]. However, there was no change in the bistable temperature range. Here we prepared a binary mixture of CCN-47 and CCN-55. The phase transition temperatures of CCN-55 are I 66 °C N 30 °C smectic-*B* (Sm-*B*), and it (CCN-55) is a homologue of CCN-47. CCN-55 also exhibits a discontinuous anchoring transition on CYTOP coated substrates with a bistable range of about 9 °C. Although the bistable range is wider than that of CCN-47, the main disadvantage is that the planar to homeotropic transition occurs in the Sm-*B* phase. Hence we prepare binary mixtures of these two compounds. Figure 8 shows the phase diagram with the bistable temperature

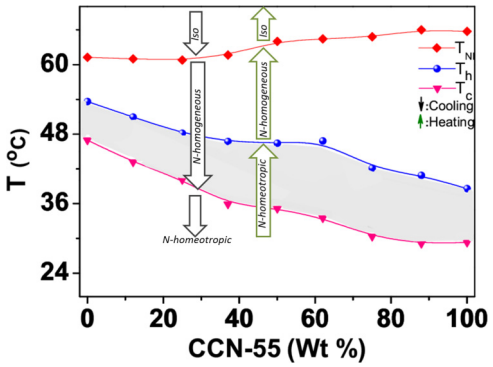

FIG. 8. (Color online) Phase diagram of a binary mixture composed of CCN-47 and CCN-55. The shaded area represents the bistable region where both the homeotropic and planar orientations are stable.

range. It is observed that the largest bistable temperature range (≈13 °C) is obtained in the mixture with 62 wt % of CCN-55. This is about 2.5 times larger than the bistable range of pure CCN-47. In addition, the bistability occurs in the *nematic* phase near room temperature. Finally, we would like to mention that the photothermal switching is an experimental demonstration of reorientation of PANI nanofibers by nematic director reorientation. The absolute values of the conductivities have to be increased several orders of magnitude for any practical application.

IV. CONCLUSION

In conclusion, we prepared liquid crystal conducting polymer nanocomposites, and our results suggest that the polyaniline nanofibers are aligned in the direction of the nematic director. In the nanocomposites, both the dielectric anisotropy and conductivity anisotropy are increased, but in the latter one the enhancement is significantly large. The bistable orientation of the nanofibers is achieved by the temperature driven anchoring transition of the host liquid crystal. In the bistable region we demonstrated a photothermal switching of the nanofibers from vertical to planar. The bistable temperature range in the nematic phase is enhanced 2.5 times in a binary mixture.

ACKNOWLEDGMENTS

We gratefully acknowledge financial support from DST (SR/NM/NS-134/2010), CSIR [03(1207/12/EMR-II)], UPE-II (UoH), and Ashai Glass, Japan, for CYTOP. We thank Dr. V. S. R. Jampani for useful discussions.

[1] P. G. de Gennes, *The Physics of Liquid Crystals* (Clarendon, Oxford, 1993).
[2] K. Takatoh, M. Hasegawa, M. Koden, N. Itoh, R. Hasegawa, and M. Sakamoto, *Alignment Technologies and Applications of Liquid Crystals* (Taylor and Francis, London and New York, 2005).
[3] *Liquid Crystals: Applications and Uses*, edited by B. Bahadur (World Scientific, Singapore, 1990), Vol. 1.
[4] J. Niitsuma, M. Yoneya, and H. Yokoyama, Appl. Phys. Lett. **92**, 241120 (2008).
[5] J. S. Gwag, J. H. Kim, M. Yoney, and H. Yokoyama, Appl. Phys. Lett. **92**, 153110 (2008).
[6] G. D. Boyd, J. Cheng, and P. D. T. Ngo, Appl. Phys. Lett. **36**, 556 (1980).
[7] D. W. Berreman and W. R. Heffner, J. Appl. Phys. **52**, 3032 (1981).
[8] H. Ong, R. B. Meyer, and A. Hurd, J. Appl. Phys. **55**, 2809 (1984).
[9] R. Barberi, M. Boix, and G. Durand, Appl. Phys. Lett. **55**, 2506 (1989).
[10] J. H. Kim, M. Yoneya, J. Yamamoto, and H. Yokoyama, Appl. Phys. Lett. **78**, 3055 (2001).
[11] P. C. Schuddeboom and B. Jerome, Europhys. Lett. **39**, 515 (1997).
[12] M. Yoneya, J. H. Kim, and H. Yokoyama, Appl. Phys. Lett. **80**, 374 (2002).
[13] D. Andrienko, A. Dyadyusha, Y. Kurioz, V. Reshetnyak, and Y. Reznikov, Mol. Cryst. Liq. Cryst. Sci. Technol., Sect. A **321**, 299 (1998).
[14] I. B. Altfeder and D. M. Chen, Phys. Rev. Lett. **84**, 1284 (2000).
[15] H. Carchano, R. Lacoste, and Y. Segui, Appl. Phys. Lett. **15**, 414 (1971).
[16] R. S. Potember, T. O. Poehler, and D. O. Cowan, Appl. Phys. Lett. **34**, 405 (1979).
[17] J. Miller, Angew. Chem. **42**, 27 (2003).
[18] B. Y. Yang, J. Ouyang, L. Ma, R. J. Tseng, and C. W. Chu, Adv. Funct. Mater. **16**, 1001 (2006).
[19] L. P. Ma, J. Liu, and Y. Yang, Appl. Phys. Lett. **80**, 2997 (2002).
[20] R. Basu and G. S. Iannacchione, Phys. Rev. E **81**, 051705 (2010).
[21] M. Rahman and W. Lee, J. Phys. D **42**, 063001 (2009).
[22] M. D. Lynch and D. L. Patrick, Nano. Lett. **2**, 1197 (2002).
[23] S. Sridevi, S. K. Prasad, G. G. Nair, V. D'Britto, and B. L. V. Prasad, Appl. Phys. Lett. **97**, 151913 (2010).
[24] R. Basu and G. S. Iannacchione, Phys. Rev. E **80**, 010701(R) (2009).
[25] R. Manda, V. Dasari, P. Sathyanarayana, M. V. Rasna, P. Paik, and S. Dhara, Appl. Phys. Lett. **103**, 141910 (2013).
[26] S. Dhara, J. K. Kim, S. M. Jeong, R. Kogo, F. Araoka, K. Ishikawa, and H. Takezoe, Phys. Rev. E **79**, 060701(R) (2009).
[27] T. A. Kumar, P. Sathyanarayana, V. S. S. Sastry, H. Takezoe, N. V. Madhusudana, and S. Dhara, Phys. Rev. E **82**, 011701 (2010).
[28] S. Aya, Y. Sasaki, D. Pociecha, F. Araoka, E. Gorecka, K. Ema, I. Musevic, H. Orihara, K. Ishikawa, and H. Takezoe, Phys. Rev. E **89**, 022512 (2014).
[29] M. Uehara, S. Aya, F. Araoka, K. Ishikawa, H. Takezoe, and J. Morikawa, Chem. Phys. Chem. (2014), doi:10.1002/cphc.201300975.
[30] J. K. Kim, F. Araoka, S. M. Jeong, S. Dhara, K. Ishikawa, and H. Takezoe, Appl. Phys. Lett. **95**, 063505 (2009).
[31] J. K. Kim, K. V. Le, S. Dhara, F. Araoka, K. Ishikawa, and H. Takezoe, J. Appl. Phys. **107**, 123108 (2010).
[32] T. A. Kumar, K. V. Le, S. Aya, S. Kang, F. Araoka, K. Ishikawa, S. Dhara, and H. Takezoe, Phase Trans. **85**, 888 (2012).
[33] V. S. R. Jampani, M. Skarabot, H. Takezoe, I. Musevic, and S. Dhara, Opt. Express **21**, 724 (2013).
[34] S. Dhara and N. V. Madhusudana, Europhys. Lett. **67**, 411 (2004).
[35] S. Dhara and N. V. Madhusudana, Europhys. J. E **13**, 401 (2004).
[36] S. Dhara and N. V. Madhusudana, Phase Trans. **81**, 561 (2008).
[37] P. Paik, R. Manda, C. Amgoth, K. S. Kumar, RSC Adv. **4**, 12342 (2014).
[38] A. I. Goncharuk, N. I. Lebovka, L. N. Lisetski, and S. S. Minenko, J. Phys. D **42**, 165411 (2009).